Effects of Structure Height on Seismic Demands of Weak and Under-designed RC Frames Considering Soil-Structure Interaction

Behtash JavidSharifi [a], Gholam Reza Atefatdoost [b,*]

[a] *Design & Development Department, Fars Regional Electric Company, Shiraz, Iran*

[b] *Department of Civil Engineering, Islamic Azad University, Estahban, Iran*

Abstract

Existing under-designed structures, which have been built due to the past insufficient constructional knowledge, are an important issue and anticipation of their dynamic responses to seismic events may be a cumbersome task. It is crucial to account for seismic demands of such structures for later retrofitting plans. In this research, three under-designed RC frames with different heights are considered to represent low-, mid- and high-rise structures. By performing non-linear response analyses, maximum seismic demands are calculated subject to five earthquake motions considering soil-structure interaction. The structures are designed for gravity loads and, especially for the high-rise, they lack about 30 percent rebar with respect to requirement for equivalent Special Moment-Resisting Frames. The major factors controlling the results are the input motion and soil conditions. The maximum inter-story drifts differ and critical stories shift upward or downward and may violate code-provided limits when the underlying soil state changes. Judgment can be made about the effects of loose and medium-dense underlying soils on structural responses. The critical sub-soils for low- and high-rise structures are medium-dense and loose sands, respectively. Subject to one single record, when the structure is high-rise, the maximum base shear is bigger with the base of the structure being flexible. For weak low- and mid-rise flexible-base structures, compared to the fixed-base state, the base shear is always smaller. The peak roof acceleration is generally greater than peak ground and bedrock accelerations, with exceptions in low-rise flexible-base structures.

Keywords: Soil-Structure Interaction, Seismic Demand, RC Frame, Structure Height

1. Introduction

It has been observed that structural responses do not only depend on the super-structure characteristics, especially when the structure is subjected to dynamic loads (e.g. [1 & 2]). When the source of the dynamic load imposes the motions to affect the structure through the underlying ground, this effect of Soil-Structure Interaction (SSI) is more accentuated. Nevertheless, according to Kausel (2010), the effect of soil on structural responses has long been known [3]. This effect has raised the interest of engineers and researchers mainly after massive structures on sites with loose soils emerged in constructions. After the importance of the issue became clear following such events as the Northridge earthquake (Northridge, USA, 1994) and ever since computational devices permitted, the conventional studies on structural responses evolved and this interdisciplinary subject was accounted for in most structural engineering problems. Fragility and vulnerability of structures have been under study taking into account possible flexibility of the foundation (e.g.[4-7]). The latter has also attracted the attention of researchers in terms of structural and geotechnical design (e.g. [8-11]). Soil-structure interaction (SSI) is effective and important in structural control (e.g. [12-14]). It has been observed that overall seismic responses of structures may also considerably change compared to fixed-base states (e.g. [1, 15-18]). Additionally, comparisons have been made in the literature among different methods of modeling the media for the sake of SSI analysis and new techniques are still being offered (e.g. [19-27]) which comprises a large deal of the researches done in this field. A comprehensive review of the history of SSI from the very beginning was given by Kausel (2010). Dynamic structure-soil-structure interaction (SSI) is one other rather newer field of SSI which has recently attracted the attention of and

✉ *Corresponding Author: Email Address: gh_atefatdoost@iauest.ac.ir*

is of growing interest to researchers (e.g. [28-38]). Soil-structure interaction analysis is mainly carried out through two approaches, namely the sub-structuring method and the rigorous. A comprehensive and detailed account of the former was presented by Wolf (1985) and Wolf (1988) [39 & 40], while the rigorous method has been of more interest in more researches due to its preciseness and plausibility [41].

All structures are supported by the ground and the ground is not always rigid. While effort may be put to properly stabilize the site soil before construction is started, subject to the weight of the structure and possible dynamic loads, the base of the structure may reveal flexibility with respect to the incoming loads. It can be ascertained that there will eventually be a depth at which the soil is either so compact that behaves essentially rigidly or there lies the rigid or rigid-like bedrock through which the earthquake motion is conveyed toward the structure. There will then be the soil through which the motion reaches the structure which affects the earthquake motion, changing it to the so-called effective input motion. Delivered to the surface of the ground, this input motion is exerted to the foundation of the structure on which the structure is expected to stand soundly. It, hence, seems at times too crude to overlook the role of the site soil and assume all structures to bear earthquake loads directly from a rigid bedrock.

While dynamic behavior of structures can be efficiently assessed considering different aspects that might affect the behavior of the structure, and although advanced methodologies exist to account for retrofitting of under-designed structures (e.g. [42-44]), it seems to be essential to carry out research to figure out global weaknesses of structures that have not been designed for lateral loads when they are subject to seismic SSI. Seismic behavior of these structures has been of interest (e.g. [45 & 46]), but non-linear dynamic analysis considering the soil-structure system is still important to be studied.

The aim of this treatment is to perform a concise yet reliable study of dynamic SSI effects on responses and seismic demands of under-designed structures considering the most prominent features of the media and outputs. Effort has been put on capturing the effects of foundation flexibility induced by deformability of medium-dense and loose underlying soils on those aspects of structural behavior that are easy to monitor, record and discuss. To avoid dealing with large amounts of data, three under-designed Reinforced Concrete (RC) frames are chosen each placed once on rigid ground and once on medium and loose soils subject to five earthquake motions. The structures are weak compared to requirements of ACI 318-14 [66] subject to loading requirements of ASCE 7-10 [71]. Maximum inter-story drifts, frame peak displacement profiles, maximum base shears and peak bedrock, ground and roof accelerations for each case are drawn and compared. The media (i.e. structures and the underlying soil strata) are modeled and analyzed in OpenSees 2.5.0. While foundation flexibility and soft soil effects have already been studied for design of tall structures (e.g. [47]), the major aim of this study is to find the most vulnerable parts or members of under-designed reinforced concrete (RC) structures with different heights situated on different soil types when they are subject to seismic loads, and how effective the structure height may be on its interaction with the underlying soil. Damage patterns are monitored to figure out whether changes occur when the characteristics of the soil differ. The inter-dependencies of earthquake records, structural properties and soil characteristics are investigated and discussed to reach a decent judgment on SSI effects on failure mechanism of the structure for future retrofit purposes. In short, the three factors of site soil, structure height and earthquake record have been considered to be the governing issues of structural responses and vulnerability.

2. Modeling and Analysis

Three RC frames with different heights (i.e. 3, 7 and 15 stories) were assumed on three different bases. The soil-structure systems were modeled in the finite element-based program OpenSees. Fig. 1 schematically illustrates how the domains are assumed when the rigorous SSI analysis approach is taken, as well as the details considered and modeled
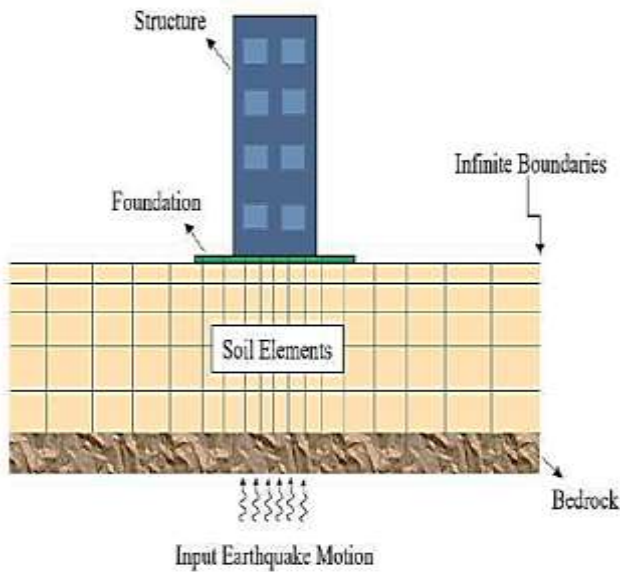
Fig 1. Elements of the media in rigorous SSI analysis approach [52]

in the present study. Fig. 2 illustrates the OpenSees models. The underlying soil is once assumed to be in medium and once in the loose state.
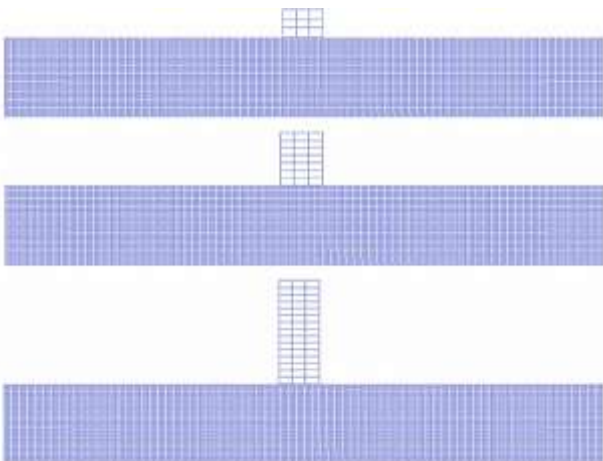
Fig 2. Selected RC frames in the soil-structure systems: (a) Low-rise: 3-story frame; (b) Mid-rise: 7-story frame; (c) High-rise: 15-story frame

2.1 Structural Elements and Properties

The moment resisting frames were assumed to meet the minimum design criteria of ACI 318-14 [66] and ASCE 7-10 [71], under distributed dead and live loads of 6.0 kN/m^2 and 2.0 kN/m^2, respectively. The plans of all three structures were regular (symmetric and three bays by three bays) so that no torsional behavior would be expected under lateral loads. Selected middle frames were then modeled in the OpenSees software. All frames have three five-meter width bays and the height of all stories is 3 meters. Table 1 presents fundamental properties of the three structures and Table 2 and Table 3 give the details of the beams and columns of the frames. In these two tables, b and h represent dimensions of the members cross sections, all with square shapes.

To model the beams and columns of the frames, the *forceBeamColumn* command was used which accounts for distributed plasticity through fiber sections and is based on the iterative force-based formulation [48-51]. Since the materials need to have the possibility of non-linear behavior, in the reinforced concrete members OpenSees built-in material models Steel01 and Concrete01 were applied for modeling the steel rebar and concrete material of the elements. Fig. 3 represents the stress-strain behaviors of these materials [48]. Tables 4 and 5 give material mechanical properties assumed in this study.

The viscous damping of the structures was accounted for using the OpenSees *Rayleigh* command which incorporates Rayleigh damping to the dynamic characteristics of the structure. The overall damping ratios for the first and third modes of vibration, which were attributed to mass-proportional and stiffness-proportional damping of
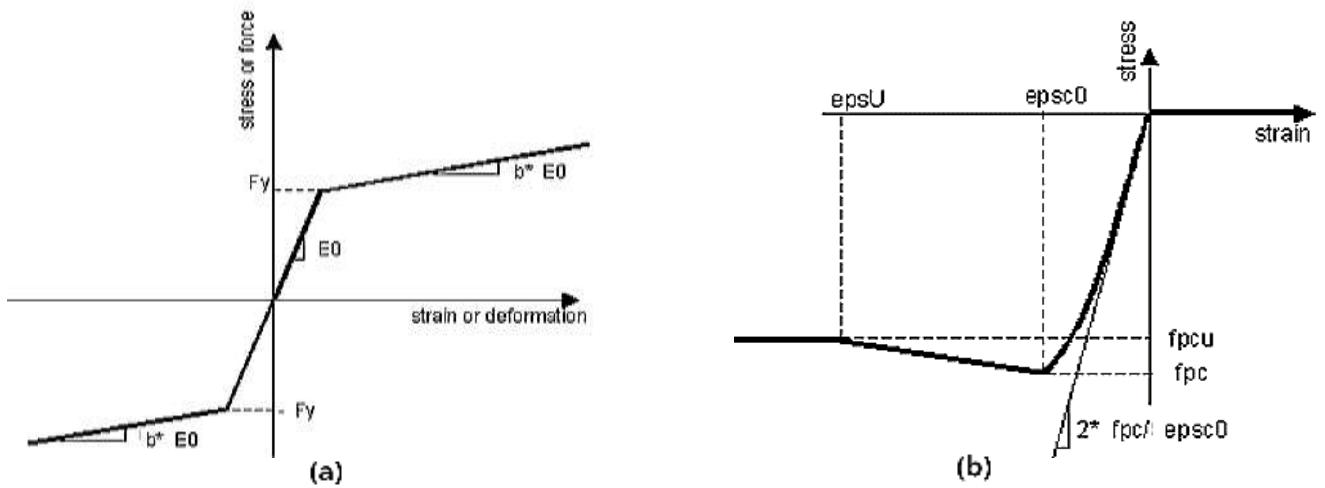
Fig 3. Stress-strain behaviors: (a) concrete; (b) steel (epsU: concrete strain at crushing strength; epsc0: concrete strain at maximum strength; fpcu: concrete crushing strength; fpc: concrete compressive strength at 28 days; Fy: yield strength; E0: initial elastic tangent; b: strain-hardening ratio (ratio between post-yield tangent and initial elastic tangent)) [48]

Table 1
Fundamental properties of the three structures

Frame/Property	Number of Stories	Total Height (m)	Fixed-base Fundamental Period (sec)	Fundamental Period with SSI (Medium Soil) (sec)	Fundamental Period with SSI (Loose Soil) (sec)
3-story	3	9	0.507	0.606	0.720
7-story	7	21	0.768	0.821	1.032
15-story	15	45	1.430	1.690	2.016

Table 2
Details of the beams

Bottom Rebar (mm)	Top Rebar (mm)	Cover to bar center (mm)	b×h (mm²)	Frame/Property
3 Φ 14	3 Φ 14	60	400×400	3-story
4 Φ 14	4 Φ 14	60	600×600	7-story
4 Φ 14	4 Φ 14	60	600×600	15-story

Table 3
Details of the columns

Rebar (%)	Rebar Size (mm)	Cover to Bar Center (mm)	b×h (mm²)	Frame
2.46	8 Φ 25	60	400×400	3-story
1.39	12 Φ 25	60	650×650	7-story
1.17	24 Φ 25	60	1000×1000	15-story

Table 4
Mechanical properties of concrete for non-linear structural modeling

Concrete Mechanical Properties	Characteristic Strength (MPa)	Strain in Maximum Strength	Crushing Strength (MPa)	Strain before Crushing	Tension Strength (MPa)
Core	25	0.0024	5.6	0.015	0
Cover	21	0.002	5	0.005	0

Table 5
Mechanical properties of steel for non-linear structural modeling

Mechanical Properties	Yield Stress (MPa)	Initial Modulus of Elasticity (GPa)	Strain Hardening Ratio (%)
Reinforcing Steel	420	200	1

2.2 Near-Field

To model soil media with finite elements, a proper soil constitutive model shall be used that can match with the problem's assumptions. Numerous models have been proposed considering certain conditions of a specific problem and bringing into account special characteristics of the soil under specifically prescribed loads (e.g. [53]). In this study, the underlying soil was modelled with the UCSD Soil Model through the OpenSees *PressureDependMultiYield* command, which defines the soil by a pressure dependent multi-yield surface constitutive model, in which the soil behavior may depend on the soil elements ambient effective pressure, which is characteristic of sandy soils. However, to strictly bind the responses to the

effective stress and assume pore water pressure build-up to control this medium, special configurations shall be met in the constitutive model. Since this (i.e. effects of liquefaction-prone soils on structural responses subject to seismic loads) is out of the scope of this research, the mentioned soil model has been used in a natural context to simply capture the elastoplastic foundation flexibility without exceptional deformations caused by soil liquefaction. This assumption can be true when the site is controlled to omit this possibility, e.g. through implementation of sufficient drainage. Fig. 4 depicts the typical stress-strain behavior of the soil material, and the mechanical properties of the two soil types are given in Table 6.
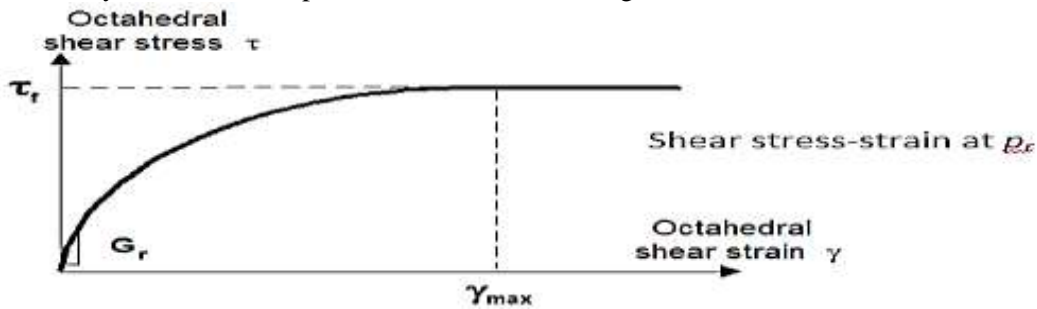
Fig 4. Shear stress-shear strain behavior of UCSD soil [48 & 57]

Table 6
Sand properties used in the numerical simulations

Soil State	Mass Density (ρ) (Ton/m^3)	Reference Shear Modulus (G_r) (MPa)	Reference Bulk Modulus (B_r) (Mpa)	Friction Angle (Φ) (degrees)	Phase Transformation Angle (Φ_{PT}) (degrees)	Peak Shear Strain (γ_{max}) (-)	Reference Pressure (p_r) (kPa)	Pressure Dependence Coefficient (d) (-)	Initial porosity $\in$ (-)
Medium	1.9	750	200	33	27	0.1	80	0.5	0.7
Loose	1.7	550	150	29	29	0.1	80	0.5	0.85

In Fig. 4, G_r is reference (low-strain) shear modulus, specified at a reference mean effective confining pressure (p_r). γ_{max} is an octahedral shear strain at

which the maximum shear strength is reached, specified at p_r. Octahedral shear strain is defined as:

$$\gamma = \frac{2}{3}[(\zeta_{xx} - \zeta_{yy})^2 + (\zeta_{yy} - \zeta_{zz})^2 + (\zeta_{xx} - \zeta_{zz})^2 + 6\zeta_{xy}^2 + 6\zeta_{yz}^2 + 6\zeta_{xz}^2]^{\frac{1}{2}} \tag{1}$$

where ξ_{ij} are strains parallel to the j and normal to the i directions and p_r is accordingly the reference normalizing pressure at which G_r and γ_{max} are defined. The octahedral shear stress, i.e. the vertical axis in Fig. 4, is defined as:

$$\tau = \frac{1}{3}[(\sigma_{xx} - \sigma_{yy})^2 + (\sigma_{yy} - \sigma_{zz})^2 + (\sigma_{xx} - \sigma_{zz})^2 + 6\sigma_{xy}^2 + 6\sigma_{yz}^2 + 6\sigma_{xz}^2]^{\frac{1}{2}} \tag{2}$$

σ_{ij} being effective stresses parallel to the j and normal to the i directions. At a constant confinement p', the shear stress τ (octahedral) - shear strain γ (octahedral) non-linearity is defined by a hyperbolic (backbone) curve:

$$\tau = \frac{G\gamma}{1 + \frac{\gamma}{\gamma_r}\left(\frac{p_r}{p'}\right)^d} \tag{3}$$

where d is a positive constant defining variations of G as a function of instantaneous effective confining pressure p' (see Table 6). The friction angle controls the peak (octahedral) shear strength τ_f as a function of current effective confinement p':

$$\tau_f = \frac{2\sqrt{2}\sin\varphi}{3 - \sin\varphi}p' \tag{4}$$

The modulus reduction curve in the constitutive model depends on the pressure-dependence coefficient d, as in Equation 5 ([54-59]):

$$G = G_r\left(\frac{p'}{p_r}\right)^d \tag{5}$$

As was mentioned in Section 2.1, the design site class had been chosen so as to make it possible for the underlying soil to be considered as the interface of soil types D and E. This is why the V_s resulting from the reference shear moduli may seem rather high for the loose soil and rather low for the medium-density soil. For instance, the given

reference shear modulus in Table 6 results to a reference V_s equal to 569m/s for the loose soil which is a rather high value for such a soil. The accuracy of the responses from finite element analyses depends on the dimensions of the elements.

It has been shown that the maximum dimension of the elements shall not exceed one-eighth to one-fifth of the shortest wavelength used in the analyses ([60-62]). To calculate wavelength, Equation 6 can be used:

$$\lambda = \nu T \tag{6}$$

υ being the velocity at which the wave propagates and T denoting the period. Equations 7 can be used for propagation velocity of shear and longitudinal waves:

$$v_s = \sqrt{\frac{G}{\rho}} \tag{7-a}$$

$$v_p = \sqrt{\frac{E}{\rho}} \tag{7-b}$$

where v_s and v_p stand for shear and longitudinal waves, respectively, and G and E are the elastic shear and Young's moduli, respectively, and ρ is the soil density [43]. Shear waves are of higher engineering importance in earthquake motions. Also, seismic responses of soils and structures are mostly influenced by input frequencies of up to 15 to 20 Hz. Moreover, assuming the properties of the loose soil of this study, the shear wave velocity would be 180 m/sec which after multiplying by the period of 0.05 sec (corresponding to 20Hz frequency), would give the minimal wavelength equal to 9 meters. Hence, 1×1 m2 four-node quadrilateral elements were used to mesh the near-field soil media under the foundation. For this purpose the OpenSees *FourNodeQuad* element object was utilized which uses a bilinear isoparametric formulation. Thus, by using this type of element, both pressure and body forces participate in computation of consistent nodal loads [48].

2.3 Far-Field and the Fictitious Boundary

The meshed near-field soil under the structure is a homogeneous with dimensions of layer 220m long and 30m thick. The bedrock is supposed rigid [63] and *elasticBeamColumn* elements have been used at the interface of the super-structures (frames) and the sub-structure (soil). The stiffness of the *elasticBeamColumn* elements is set to be toward infinity and its DOFs are bound to the soil surface at the common nodes using the *equalDOF* command [64]. The fictitious boundary separating the near-field from the far-field is modeled using absorbent elements that damp the motions as if they are radiated to infinity [65].

2.4 Earthquake Records and Dynamic Analyses

In order to record and judge on the structural responses with respect to the different site conditions, non-linear Time History Analyses (THA) are performed. The random nature of an earthquake record, however, makes it insufficient to inspect the vulnerability of a structure through one single THA. As a result, five different earthquake motions recorded on rock are selected in order to cover a suitable range of possible strong motion characteristics. The basis of selection of the records has been to try to include different high-seismicity regions with various strong motions in the study. Therefore, famous records from a high-seismicity region of Europe (Italy), two from Asia (Turkey and Iran) and two from the US (Loma Prieta and Northridge) were applied to account for the variability of earthquake motions as a result of possibly effective site differences. Table 7 presents the earthquake records and their specifications.

Table 7
Used earthquake records

Motion Name	Date and Location	Original PGA (g)	Duration (sec)	Original Predominant Frequency (Hz)
Friuli	Friuli, Italy, 1976	0.36	36	2.00
Kocaeli	Izmit, Kocaeli, Turkey, 1999	0.26	28	1.88
Loma Prieta	Loma Prieta, Gilroy, U.S., 1989	0.22	39	1.39
Northridge	Northridge, U.S., 1994	0.15	40	2.56
Tabas	Tabas, Iran, 1978	0.85	33	1.32

3. Results and Discussion

The dependency of the behaviors of the under-designed structures on their height and site characteristics has been herein mainly monitored by recording three major responses, namely maximum story displacements, and maximum base shears and maximum induced accelerations. For the sake of story displacements, overall displacement amplitudes as well as maximum inter-story drifts are recorded for fixed-base, medium-density soil and loose soil states. Subject to each earthquake motion, the stories with critical drifts are singled out and alterations of the critical story when the underlying soil is changed are specified. The maximum base shears and roof accelerations, on the other hand, are recorded and compared for each frame on the three different sub-structures. Changes in maximum base shears when the underlying soil is substituted are notified and comparisons are made.In order to check whether the analyses have been performed logically with reliable results, three basic concepts were taken into consideration. First, the finite element model was assured to be reasonable in terms of mesh size. As was discussed in detail in Section 2.2 (Equations 6 and 7), the dimensions chosen for the finite

elements were neither too big nor too small, reassuring that no filtering of any constituent input frequency would occur. Second, the input motions were derived from the primary earthquake motions (i.e. the raw records used on the bedrock under the soils, after their baselines were corrected) by performing dynamic analyses on the finite element model which had already been assumed reliable. To This is while the peak acceleration is also shifted forward in time by quite a number of time steps. The logicality of the recorded input motions modified and transferred from the bedrock into the structures is a good standpoint to look over the overall outputs of a sample structure to check whether the result can conform to what is crudely expected.It is expected that the effects of SSI shall be most observable from stiff structures on loose soils. Based on the fundamental periods, the low-rise structure of this study is the stiffest and is considered to check the credibility of the results. As will be examined later in full details, all SSI effects are quite rational on the

this end, the base-line corrected motions were applied to the underlying bed rock and the motions were recorded on the surface of the soils. Fig. 5 represents the bedrock, medium-density and loose soil input motions of the five selected earthquakes.It is apparent from Fig. 5 that motions have been most magnified by the medium-density soil (shown in green).

3-story frame. When placed upon the loose soil, the fundamental period of the structure is increase by almost 25 percent relative to the fixed-base low-rise frame (Table 1). Furthermore, it will be illustrated in Section 3 that the average peak base shear of this frame is decreased by more than 30 percent subject to interaction with loose underlying soil, compared to the fixed-base state. Eventually, the displacement profiles and story drift patterns (both in average values and case by case outputs), with respect to the other states, are changed logically, with exception of the case of analysis under the Tabas record which has led to failure of the structure.
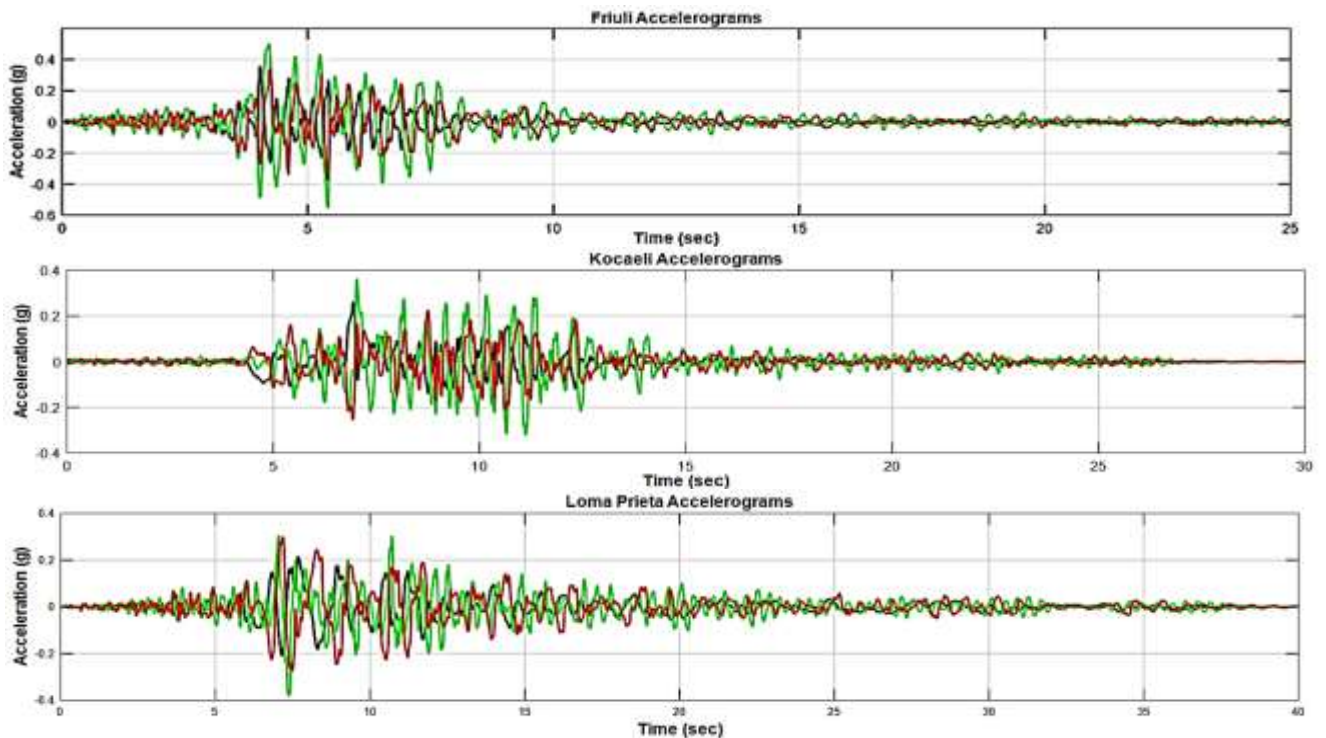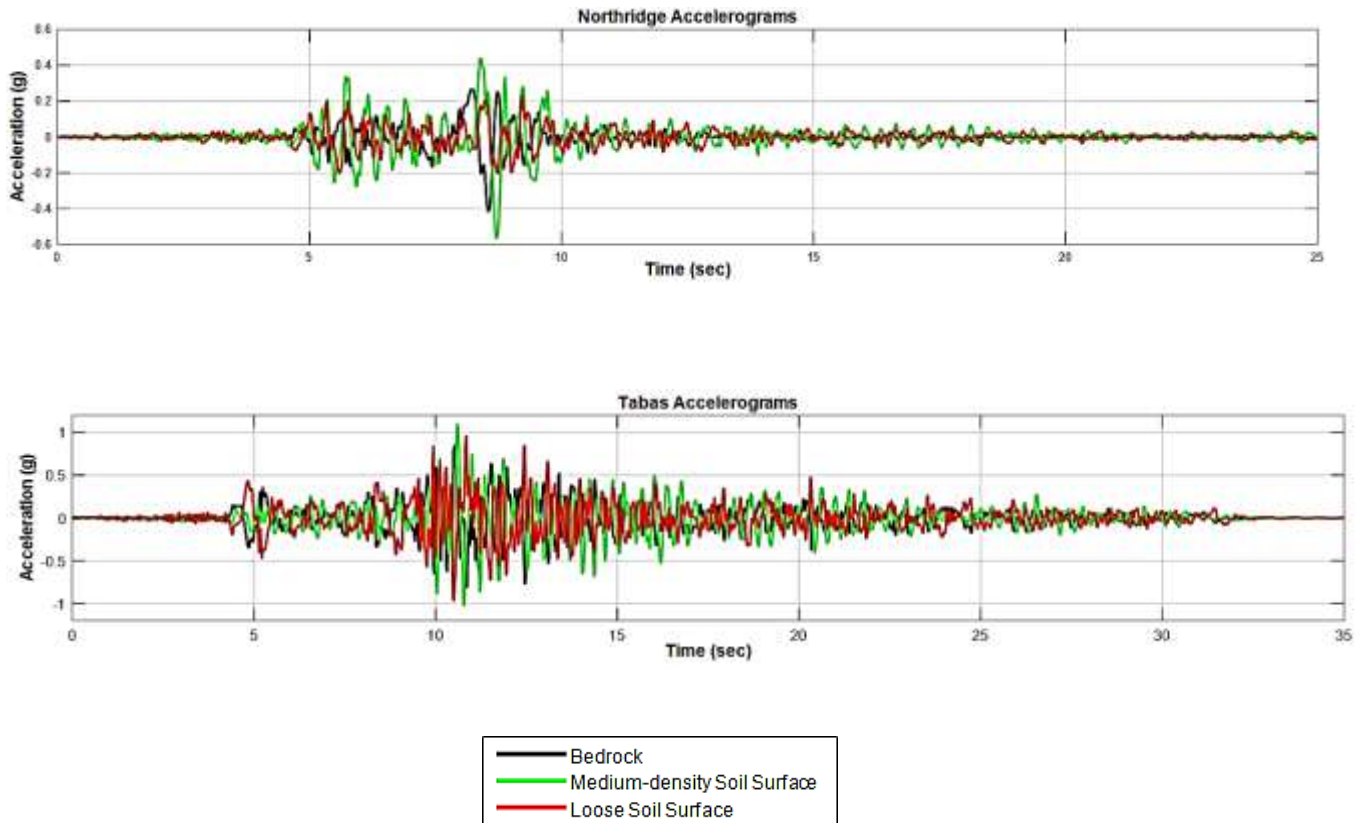
Fig 5. Primary input motions records, (a) Friuli; (b) Kocaeli; (c) Loma Prieta; (d) Northridge; (e) Tabas

3.1 Structural Drifts and Displacements

Fig. 6 depicts the maximum inter-story drift ratios of the three frames with the three different base conditions subject to the five earthquake motions. The maximum inter-story drift ratio allowed per ASCE 7-10 [71] based on which the structures were initially designed is 0.025 for low-rise and 0.02 for mid- and high-rise structures, and is shown on the diagrams with dashed magenta lines. Note shall be taken that the inter-story drifts of structures that fully or partially collapsed during dynamic analyses are only partially drawn in Fig. 6, since full unrealistically huge deformations which suggest structural collapse would lead to concealment of other drifts graphs. With regard to this figure, it is notable that Tabas earthquake has mainly been of major damage to the low-rise structure on rigid ground and medium-density soil, Loma Prieta earthquake has been of major damage to the low-rise structure on medium-density soil, Friuli earthquake has been of major damage to the high-rise structure

on rigid ground and medium density soil, Kocaeli earthquake has been of major damage to the fixed-base high-rise structure and Northridge earthquake has been of major damage to the high-rise structure on loose soil. For the three-story frame the maximum inter-story drift is at the top story for almost all non-collapsed cases except for the structure on loose soil, with a maximum of about 5% for the structure on medium-density soil subject to Northridge motion. In addition, it is observed that peak inter-story drifts are bigger for the three-story structure on medium-density soil than those on loose soil and rigid ground, which can be of significant interest, since subject to some seismic loads the peak inter-story drift may meet or surpass the maximum value allowed. In the case of Loma Prieta earthquake, beside collapse of the frame on medium-density soil, the second story of the fixed-base frame barely violates the maximum drift allowed (i.e. 2.5%).

The 7-story structure behaves more safely than the low-rise in terms of collapse, while quite a number of violations are observed. It is only subject to Kocaeli earthquake, with a maximum relative inter-story drift of 1.2% for medium-density soil state, that a safe distance between the allowed drift and the peak ones is visible.

The Friuli motion has caused the top story of the structure on medium-density soil to reach the allowable limit, whereas the bottom stories are most vulnerable to Loma Prieta earthquake, with an allowable-limit-exceeding maximum relative drift of 2.5% for the medium-density soil state at Story 3. Subject to Northridge earthquake, compared to the medium-density soil state, the critical story (i.e. Story 2) of the structure on loose soil (with a peak relative inter-story drift of 2.1%) is shifted two stories upward and its value is almost doubled. The peak relative inter-story drifts of bottom and middle stories of the frames with all base types (with maxima of 3.2% for fixed-base structure at Story 2, 3.2% at Story 3 for the structure on medium-density soil and 3.1% Story 5 of the structure on loose soil) violate the maximum prescribed drift when the structure is subjected to Tabas earthquake. It is worthwhile mentioning that it is not always necessarily one certain state that is the most critical, as, for instance, the structure on medium-density soil subject to Friuli earthquake and the one on loose soil subject to Northridge motion are of highest peak inter-story drifts.

Table 8
Changes in the location of critical stories with respect to base-underlying soil type

Tabas	Northridge	Loma Prieta	Kocaeli	Friuli	
Fixed-base Structures					
1^+, 3^+	3	2^*	3	3	3-Story
2^*	2	2^*	2	2	7-Story
6^*	5	6, 7	15^+	2^+	15-Story
Structures on Medium-density Soil					
2^+	3^*	1^+	3	3	3-Story
2^*, 3^*	2^*	3^*	5	7^*	7-Story
11	8	4^*	4, 10	3^+, $4^{+\#}$, 5^+	15-Story
Structures on Loose Soil					
1, 2	1, 2	2	2	2	3-Story
5^*	4^*	2	2	5	7-Story
13	3^+, $4^{+\#}$, 5^+	5	3-7	3, 6-10	15-Story

* Maximum relative inter-story drift allowed, which equals 0.025 for low-rise and 0.02 for mid- and high-rise structures, is violated.
+ Total structural collapse as a result of story failure
# Most critical story in terms of collapse

For the 15-story case, the Friuli earthquake has caused total demolition of the fixed-base structure and the one on medium-dense soil, which are not fully observable on the figure as a result of their far too large measures which were indicative of overall collapse. The same goes for the fixed-base high-rise structure subject to Kocaeli earthquake (Story 15) and the one on loose soil subject to Northridge motion (Story 1). Subject to Tabas earthquake, the middle stories of the fixed-base frame are also critical, with a maximum recorded relative drift of 2.5 at Story 6. All other stories of all other cases have responded safely to the five earthquakes. Note shall be taken that no shear walls had been considered to bear the lateral forces and it is merely through the moment resisting frame that these forces

are endured. It is notable that for the high-rise building subject to four of the earthquakes (excluding Tabas), whenever violations of the prescribed safe limit of inter-story drift (i.e. 2%) occurred, the utmost damage followed. Table 8 summarizes the critical stories of each frame subject to each earthquake record. Note that an asterisk suggests violation of the limit prescribed by the Standard. With regard to the used design code ACI 318-14 [66], the maximum allowed relative inter-story drift is limited to 0.025 for low-rise and 0.02 for mid- and high-rise structures. Table 8 makes it clear that the critical stories, whether or not violating the maximum allowed drift subjected to the five ground motions, are prone to change not only with change of the input motion but also with the underlying soil. The most significant point inferred from Table 8 and Fig. 6 is that when the sub-base of the mid-rise frame changes from fixed to medium-dense and flexible, the critical story which may subsequently violate the maximum drift allowed is shifted from Story 2 to stories 3, 5 or 7 for the former and to stories 4 or 5 for the latter. Additionally, for the low-rise structure, as the sub-base flexibility increases, the critical story moves downward in terms of maximum recorded relative inter-story drift, making the frame on medium-density base as the most vulnerable. For the other frames on the three base conditions subject to the five earthquakes, an erratic distribution of critical stories is observed.
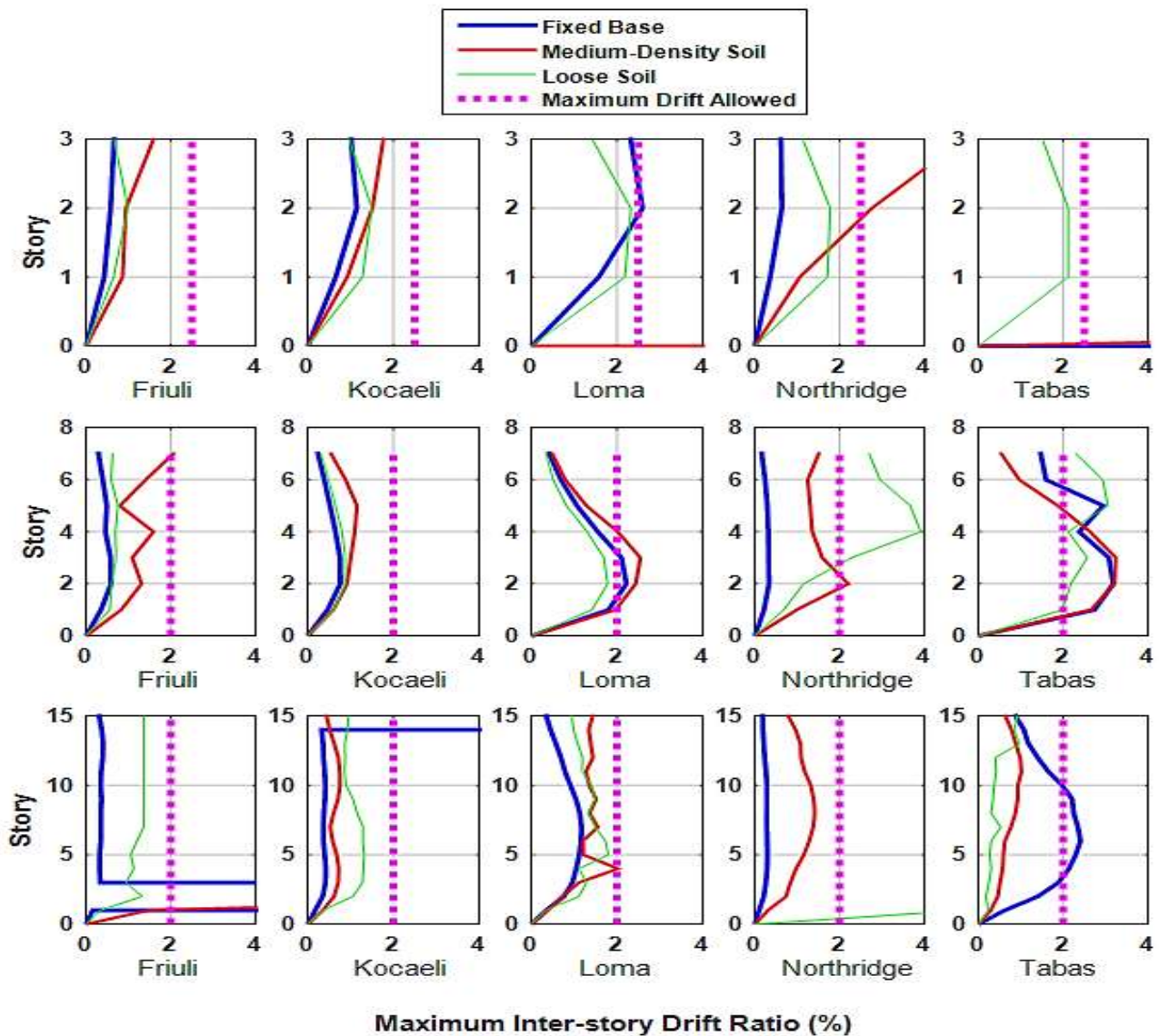
Fig 6. Height-wise distribution of maximum inter-story drift ratios, (a) Low-rise structure; (b) Mid-rise structure; (c) High-rise structure

The story displacement amplitudes are drawn in Fig. 7 for the three frames on the three base types. The effect of base displacement on overall story displacements, especially for the loose-soil state, is noticeable. In some cases (e.g. low-rise structure subject to Kocaeli and Loma Prieta motions, mid-rise structure subject to Kocaeli and Tabas motions and high-rise structure subject to Kocaeli and Loma motions) the structure on loose soil does not undergo detrimental internal deformations, yet it manifests large displacements. This can be due to the sliding of the footing of the structure owing to low shear strength of the underlying soil. This rigid-like displacement portion of the structure and its effect

on the displacement of upper stories follow rigid-body kinematic rules and is believed to depend only on geometric quantities of the structure and its foundation and not on the stiffness properties of structural elements [40]. This idea of providing the base of structures with some flexibility or possibility of rocking oscillation can be applied to mitigate structural damages (e.g. plastic hinges in columns with large irrecoverable deformations, considerable inter-story drifts, etc.) as long as it is reassured that flexibility of the base leads only to controlled deformation, triggered from mobilization of bearing capacity mechanisms under the footing [67]. It is particularly evident that in the extreme case of Tabas earthquake, the largest detrimental deformations are caused to the fixed-base structure.
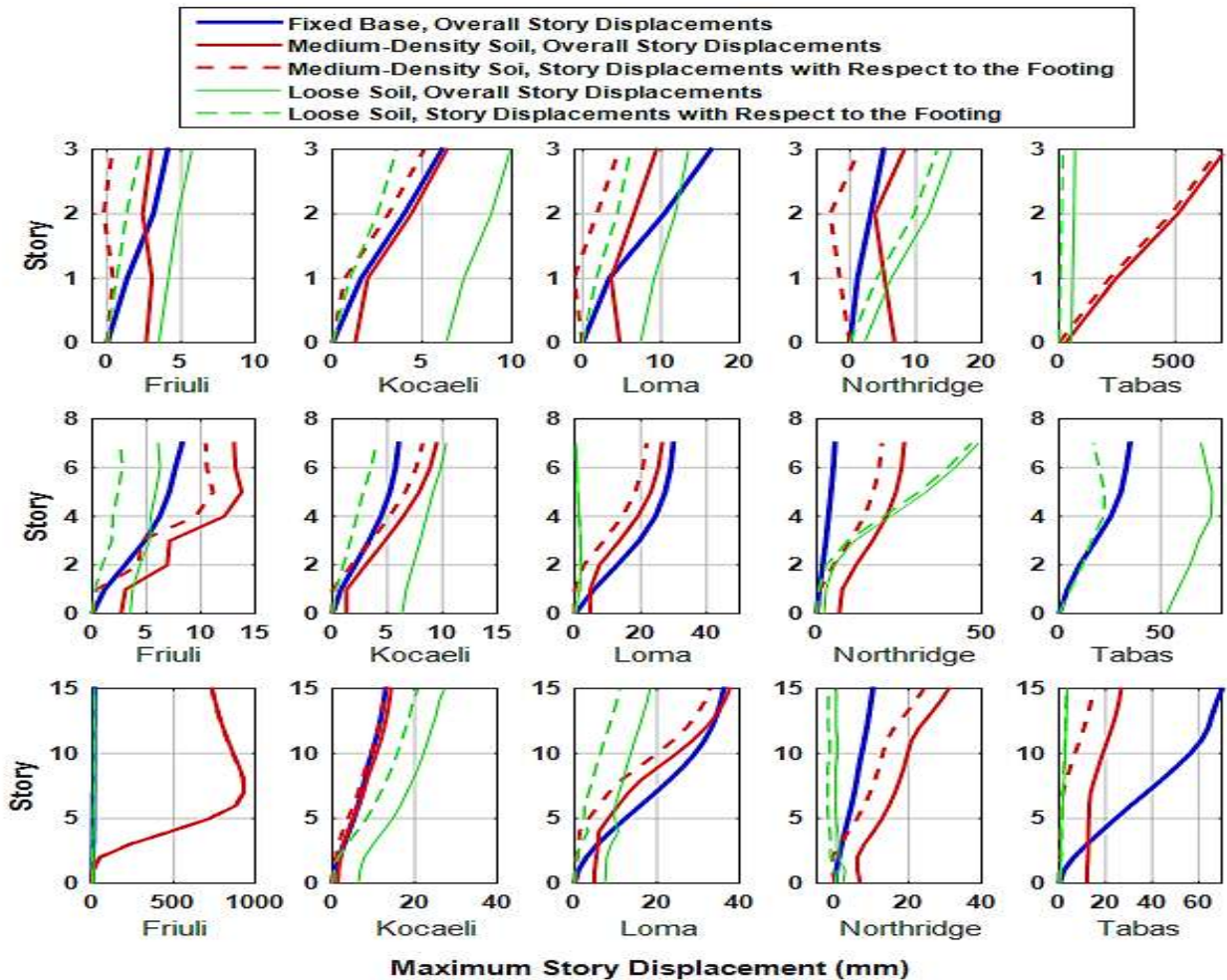
Fig 7. Total story displacement amplitudes, (a) Low-rise structure; (b) Mid-rise structure; (c) High-rise structure

Fig. 8 offers average relative inter-story drifts and story displacement amplitudes of the three structural frames (i.e. low-, mid- and high-rise) on the three base conditions (i.e. fixed, medium-density soil and loose soil). The figures imply that, in average, when the structure is assumed fixed-base, its behavior is acceptable as the average relative inter-story drifts are well behind the maximum allowed. This is while when the low-rise structure is on medium-density soil, the conditions may be different. This is also the case for the high-rise structure, which can be due to

the fact that in this state the damping of the soil is not enough to dissipate the energy of the input motion nor is the rigidity enough to restrict the deformations to a favorable limit. When the structure is high-rise, loose underlying soil may lead to the most exacting state, with an average relative inter-story drift of 28%. In short, the critical sub-structures for low- and high-rise super-structures are respectively medium-density soil and loose soil. For the mid-rise structure, medium-density soil let bottom stories meet the maximum permitted limit.
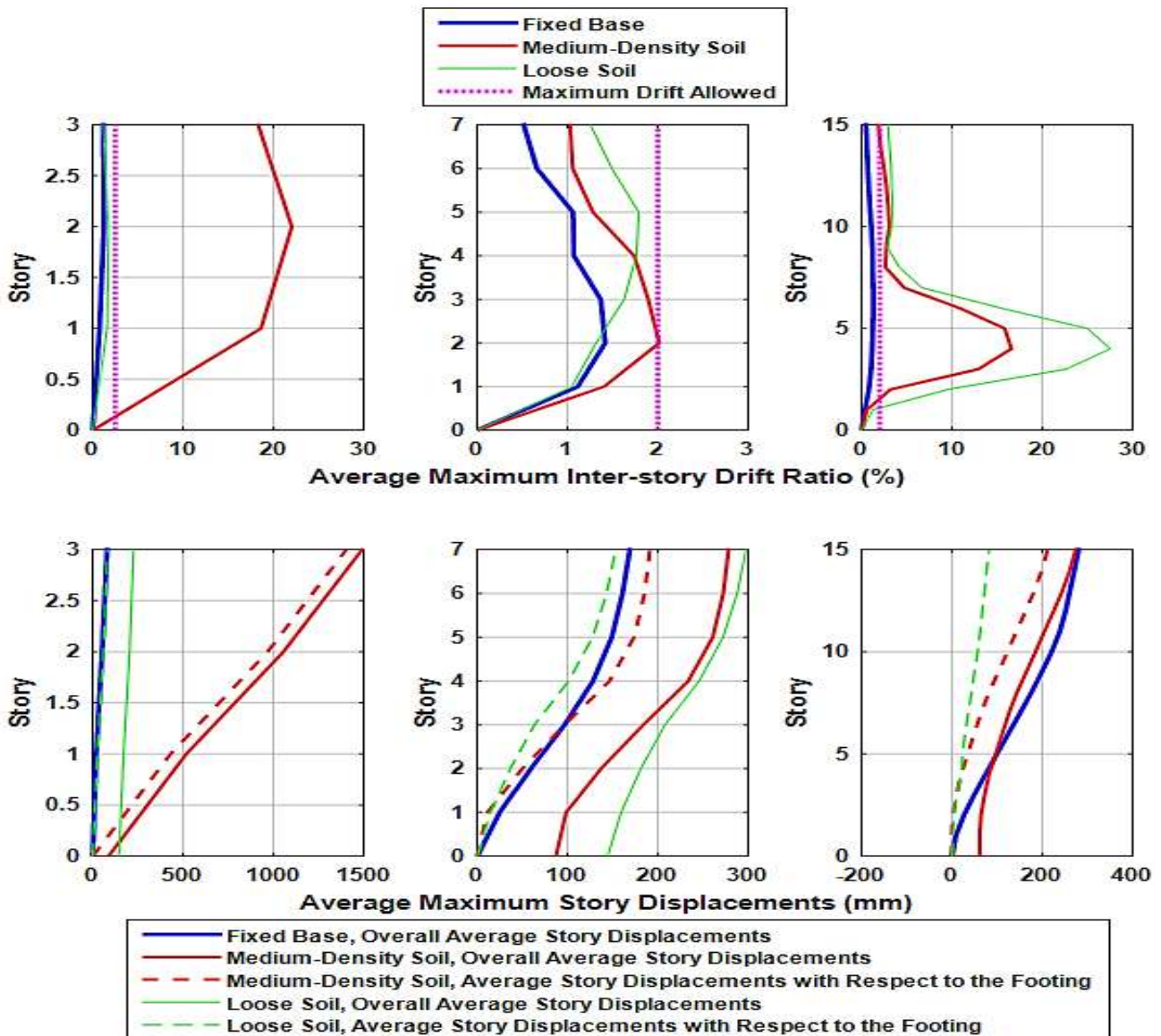
Fig 8. Average of peak story responses, (a) Height-wise distribution of relative inter-story drifts; (b) Story displacement amplitudes

3.2 Base Shears

As an account of another important measure of analysis outputs, the base shears were calculated by summing up the shears at the bottom sections of the first story columns. The peak base shears recorded for the three base states of the three frames are presented in Fig. 9. In order to investigate the effects of the structures' heights and their soil states on the induced peak base shears, comparative bar charts are included in Fig. 9 along with the overall peak shears. The peak shears are once normalized to the structures weights to reflect the effect of structure height on induced shear forces at the base of the frame (Fig. 9.b), and once compared to the maximum base shear of the fixed-base frame to represent the influence of different soil states (Fig. 9.c). It is noticed that in all cases the base shears of the structures involving SSI are smaller than what is recorded in the fixed-base case. For the case of Tabas earthquake, however, no peak base shear is reported for the fixed-base low-rise structure due to the fact that the structure collapsed totally before the seismic load was fully exerted. Numerically, this resulted in illogically huge base shears, which was indicative of numerical instability of the failing model. Hence, no comparison was possible in terms of fixed-base shears for the low-rise structure subject to Tabas record (Fig. 9.c).

It is natural for the base shear amplitudes to depend strictly on the input motion as well as on the weight of the structure. A comparison between the inter-story drifts and base shears suggests that it is not merely the pure base shear during an earthquake that determines structural damages due to inter-story drifts. Which mode of deformation is accentuated by earthquake is also an indispensable factor that depends on the natural frequencies of the structure as well as the predominant frequency range of the earthquake record. For instance, story instabilities are observable in the fixed-base high-rise structure subject to Friuli and Kocaeli motions, whilst the maximum recorded base shears for neither case exceeds 500 kN.

One other distinguishing feature of Fig. 9 is that the maximum and minimum base shear demands are those induced by the Tabas earthquake. It is of interest that while the highest recorded base shears are associated with the fixed-base structures subject to this motion, surprisingly, when the site soil state is changed to loose, the base shears are decreased by more than 90 percent. The reason of this dichotomy was found to be the failure that occurred in the sub-base soil of the structure, which halted the dynamic analysis. Although until the ninth second of the analysis the structure does not undergo considerable deformations, the large strains induced in the sub-structure lead the system to confront numerical singularities resulting in disruption and termination of the analysis before it is completed. Therefore, the results reported for the 15-story structure on medium-density and loose soils subject to Tabas record do not cover the whole range that would be expected from a complete THA. This is attributed to the intense nature of the Tabas earthquake in terms of peak accelerations and frequency content. Thus, for the structure to respond safely to an earthquake with such characteristics, it is not enough to merely make sure of structural stability and performance level; the sub-base conditions must be checked so that one can reassure no failure will therein occur. In this regard, the fixed-base state is the safest for this specific condition (i.e. high-rise structure subject to Tabas motion) after all. The change in the effective fundamental period of the high-rise structure in the soil-structure system with loose soil compared to the fixed-base structure (*see* Table 1) would also result in reduced base shears.

Table 9 presents a good account of base shear variations of the SSI-prone structures with respect to reactions of the fixed-base ones. With regard to the base shears and relative inter-story drifts, it is noteworthy that considering the effects of the site soil on dynamic responses of a structure in most cases results in decreased internal forces of the structural members, as the horizontal base reactions are reduced. The reasons of this reduction is include increased fundamental periods of the structure when it is situated on soil, the dissipation of energy by internal deformation of underlying soil elements which can damp the forces conveyed to or induced in the structure, etc. This, however, cannot guarantee that overlooking SSI will result in a safer design. The reason is that although base shears mostly reduce when the underlying soil interacts with the structure, the increased story displacements caused by induced base displacements can not only lead to differed damage patterns which shall be considered effective on the structural design, but also affect serviceability of the structure and probability of inter-structural impacts. On the other hand, it cannot be always guaranteed that base reactions are smaller subject to SSI.
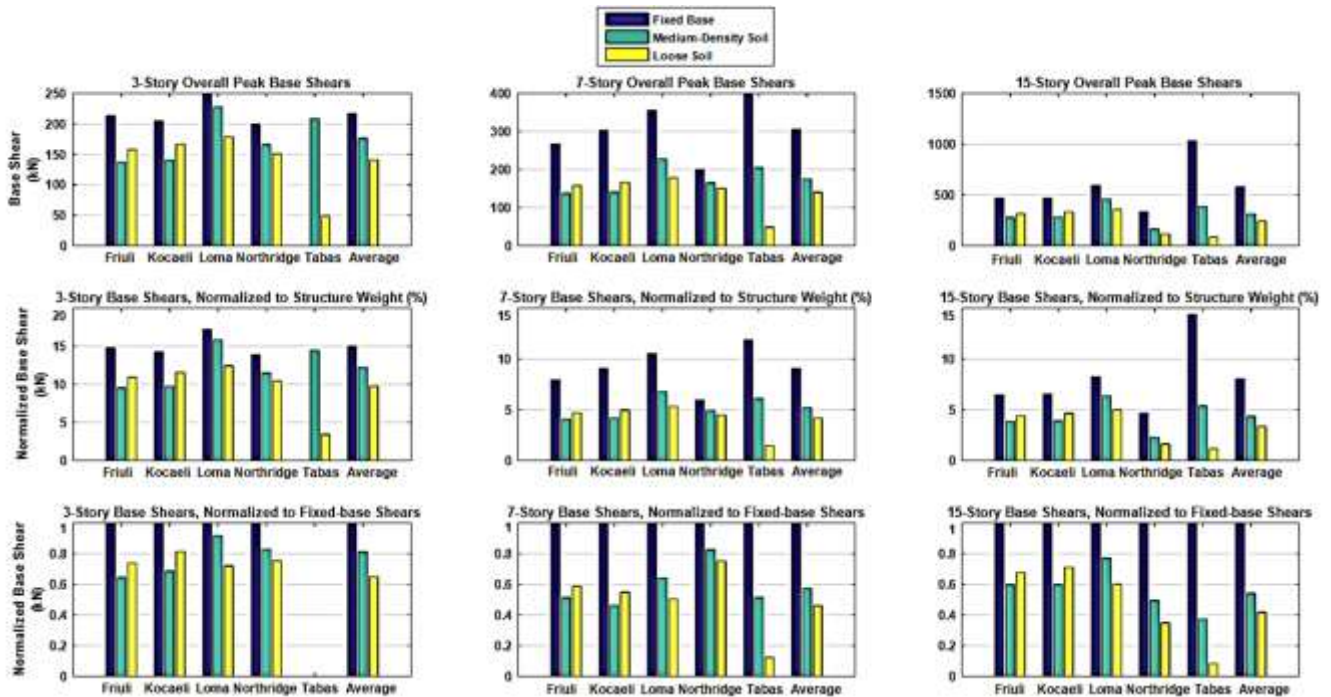
Fig 9. Comparison of peak base shears for different base conditions: (a) Overall values; (b) Values normalized to weights of structures; (c) Values normalized to the fixed-base state peak shears

3.3 Acceleration Magnification

To investigate the effects of seismic loads on soil-structure systems, it is also customary to record and monitor how peak accelerations vary from the bedrock up until the roof of the structure. These variations often make the eventual peak roof acceleration (PRA) become much greater than the peak bedrock acceleration (PBA), whose measure depends on the nature of the primary and effective input motions, the site soil and the height of the structure. Fig. 10 illustrates how the accelerations have been magnified when they travel from the bedrock up into the structural frames. These magnified peak accelerations are not shown for cases in which either the whole structure or its top story was destructed (e.g. the fixed-base low-rise frame subject to Tabas earthquake and low-rise frame on medium-density soil subject to Loma Prieta earthquake), as the unrealistic scale would conceal the visibility of other bars. Although in most cases

the differences between PRAs and peak ground accelerations (PGAs) are contrastive, it is of note that in some cases (e.g. low-rise frame on medium density and loose soils respectively subject to Friuli and Tabas earthquakes) the PGA is close the PRA. This is while in one case (i.e. 3-story frame on medium-density soil subject to Northridge earthquake) the PBA exceeds the PRA, which accounts for the considerable sliding of the footing observed in Fig. 7. In addition, for the cases of high-rise structure on medium-density and loose-soils subject to Tabas earthquake motion, the PBA is seemingly greater than PGA. This again is due to the fact that the analyses could not be completed, and no proper comparison can be made between the full bedrock accelerogram and the first nine seconds of that of the ground surface. These bars representing the PGA of Tabas earthquake motion imposed on the high-rise structure-soil system is not reliable.

Table 9
Base shear reduction ratios for different soil conditions relative to the fixed-base state (%)

Loose Soil	Medium Soil	Earthquake
Low-rise Structure		
26	35	Friuli
18.6	31.3	Kocaeli
27.9	8.1	Loma Prieta
24.6	17.1	Northridge
70	60	Tabas
35	18.7	Average
Mid-rise Structure		
41.1	48.6	Friuli
45	53.6	Kocaeli
49.6	35.8	Loma Prieta
24.8	17.3	Northridge
87	48.5	Tabas
53.8	42.5	Average
High-rise Structure		
32.3	40.2	Friuli
28.8	40	Kocaeli
39.8	22.9	Loma Prieta
65.1	50.4	Northridge
91.7	62.6	Tabas
58.2	45.8	Average

The first row of Fig. 10 illustrates magnification of accelerations when the structure is fixed-base. This is why the PBAs and PGAs are equal in Fig. 10.a. Figs. 10.b and 10.c, respectively, involve peak medium-density and loose soil accelerations. Table 10 presents the magnification factors of peak accelerations for the three frames with the three base conditions subject to the five earthquake motions.

The values presented in Table 10 are derived by dividing the PRAs and PRAs by the PBA for each earthquake motion. It is clear that in most cases the earthquake motion is magnified in terms of peak acceleration when it travels from the bedrock to the structure base. It is important to note that, the ground accelerations reported in Table 10 and Fig. 10 are those of the *'effective input motions,'* while the accelerograms depicted in Fig. 5 are 'primary input motions,' the former being the acceleration imposed to the base of the structure when obviously both super-structure and substructure are present. The latter, on the other hand, is when there is no structure on the soil layer and the motion is merely modified by passing through the soil from until it is recorded on the soil surface. Except the numerical procedure (i.e. finite element analysis) taken in this study, other methods of determining this magnification, namely the Multiplier Approach [1] and the Transfer Function Approach [41] are common which are mostly carried out in the frequency domain. It is of note that the effective input motion magnification factors reported in Table 10 are only applied on the peak accelerations, and are not constant through the acceleration histories.

With regard to Table 10, SSI effects are apparent for the peak effective input acceleration of the Northridge earthquake motion when it is exerted to the structure on medium-density soil. The magnification is clearly observable (roughly 3.8 for all frames), which well complies with the historic evidence concerning this event (e.g. [68-70]). Also, be regarded as possible peak values since they correspond to the last time step before the analysis and 9 seconds for the loose soil). note that the values reported for high rise SSI-prone structure subject to Tabas earthquake motion cannot was disrupted (15 seconds for the medium-dense soil.

Table 10
Peak roof and ground (effective input motion) accelerations relative to peak bedrock accelerations (PRA/PBA & PGA/PBA)

Sub-base with Loose Soil	Sub-base with Medium-density Soil	Roof #3	Roof #2	Roof #1	Earthquake
Low-rise Structure					
1.0671	1.5376	1.38	1.53	1.34	Friuli
0.9832	1.3194	1.65	1.85	1.44	Kocaeli
1.3207	1.8406	2.54	27.53$^+$	2.16	Loma Prieta
1.3884	3.7696	3.26	2.93	2.53	Northridge
1.1250	1.1852	1.15	1.7	$6.24\times10^{5+}$	Tabas
Mid-rise Structure					
1.0711	1.5361	3.04	2.82	2.19	Friuli
0.9828	1.3178	2.30	3.91	2.46	Kocaeli
1.3220	1.8373	3.95	4.18	3.53	Loma Prieta
1.3995	3.7737	9.30	7.95	2.96	Northridge
1.1311	1.1842	1.18	1.54	2.09	Tabas
High-rise Structure					
1.0640	1.5384	11.24	12.27	2.28	Friuli
1.0006	1.3177	13.78	4.79	4.38	Kocaeli
1.3439	1.8386	13.05	12.90	2.66	Loma Prieta
1.5908	3.7703	27.32	11.35	3.84	Northridge
0.1211	0.6851	4.40	1.37	2.63	Tabas

Roof #1: roof of structure with fixed base; Roof #2: roof of tructure on medium-density soil; Roof #3: roof of structure on soft soil
+ Illogically huge due to structural instability
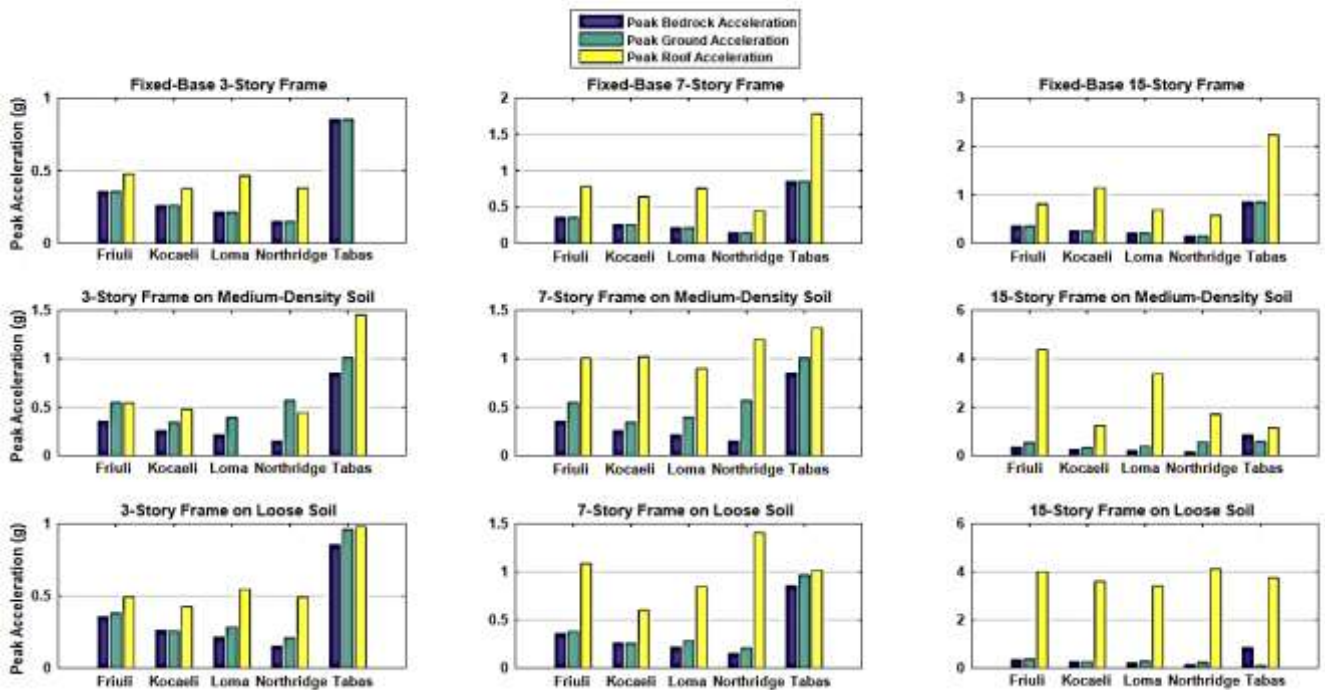
Fig 10. Magnification of peak accelerations from bedrock to roofs of (a) Fixed-base frames; (b) Frames on medium-density soil; (c) Frames on loose soil

4. Conclusions

A concise study was performed on under-designed structures encompassing most salient features of rigorous soil-structure interaction analysis for practical purposes. Three weak frames representing low-rise, mid-rise and high-rise structures were assumed to be first fixed-base and then on medium-density and loose soils subject to five earthquake motions. The bounded underlying soil was modeled with finite elements reaching a fictitious boundary separating the far-field from the near-field. The near- and far-field boundary was modeled to be absorbent by inserting radiation damping capability in order for it to play the role of infinity toward which the reflected seismic waves would travel. Story displacements and base reactions were recorded in order to capture the dependency of structural responses to site conditions. The following are the most prominent results obtained for seismically weak RC frames subject to dynamic SSI:

1- Moving from one soil state to another, the critical story may shift with regard to its location, the drift value or both.
2- In the high-rise structure on different base conditions, the displacement amplitudes of middle stories roughly coincide irrespective of the base type. In the low-rise structure, this occurs for the fixed- and medium-density-soil bases at the middle or the bottom story.
3- Relative inter-story drift, as a conventionally known damage index, does not merely depend upon the super-structure; the sub-soil may lead to unexpected variations in values of this this damage index as well as in the location of the story with the largest displacement.
4- When the underlying soil is loose, the movement of the base of low-rise structures relative to the ground results in smaller relative inter-story drifts especially during more intense earthquakes, except if the bottom stories prove to be soft. This is while drifts generally increase in flexible-base structures compared to the fixed-base state, if the structure does not collapse.
5- Subject to intense earthquakes, the maximum base shear of the structure resting on loose soil may decline to 30 percent. This accounts for the need of modeling the soil with the structure when assessing the vulnerability of the structure to dynamic loads, as not only is the damage pattern estimated more accurately this way, the real lateral forces, that may be far below those of the fixed-base structure, can yield much more economical yet safe enough design schemes.
6- There could be some cases (although rare) in which peak ground acceleration is not substantially less than peak roof acceleration. This mostly occurs in low-rise buildings on loose soils.
7- Moving from the bedrock to the roof of the structure, the peak acceleration increases. This means that in most cases where the structure resists the whole earthquake, the peak roof acceleration is higher than the peak ground acceleration, which is in turn more than the peak bedrock acceleration. Depending on the height of the structure, the difference of peak roof acceleration with the other two can be substantial. In some cases, especially for the high-rise structure, the peak recorded roof acceleration is considerably higher when the structure is prone to SSI, compared to the fixed-base structure. In short, accounting for SSI proves that real peak roofs accelerations are higher than how much they are assumed to be without SSI.

References

[1] Rahnema, H., Mohasseb, S. and JavidSharifi, B. (2016), "2-D soil-structure interaction in time domain by the SBFEM and two non-linear soil models," *Soil Dynamics and Earthquake Engineering* **88**: 152-175.

[2] Atefatdoost, Gh. R., JavidSharifi, B. and Shakib, H, (2018), "Effects of foundation flexibility on seismic demands of asymmetric buildings subject to near-fault ground motions." *Structural Engineering and Mechanics*, **66(5)**: 637-648. DOI: https://doi.org/10.12989/sem.2018.66.5.637.

[3] Kausel, E. (2010), "Early history of soil–structure interaction," *Soil Dynamics and Earthquake Engineering* **30**(9): 822-832.

[4] Behnamfar, F. and Banizadeh, M., (2016), "Effects of soil–structure interaction on distribution of seismic vulnerability in RC structures," Soil Dynamics and Earthquake Engineering Volume 80, pages 73-86.

[5] Mitropoulou, C. Ch., Kostopanagiotis, C., Kopanos, M., Ioakim D. and Lagaros, N. D.

(2016), "Influence of soil–structure interaction on fragility assessment of building structures," *Structures* **6**: 85-98.

[6] Mekki, M., Elachachi, S.M., Breysse, D. and Zoutat, M. (2016), "Seismic behavior of R.C. structures including soil-structure interaction and soil variability effects," *Engineering Structures* **126**(1): 15-26.

[7] Hokmabadi, A.S., Fatahi, B. and Samali, B. (2014), "Assessment of soil–pile–structure interaction influencing seismic response of mid-rise buildings sitting on floating pile foundations," *Computers and Geotechnics* **55:** 172-186.

[8] Atefatdoost, Gh. R., Shakib, H. and JavidSharifi, B. (2017), "Distribution of strength and stiffness in asymmetric wall type system buildings considering foundation flexibility," *Structural Engineering and Mechanics*, **63**(3): 281-292.

[9] Lu, Y., Hajirasouliha, I. and Marshall, A. M. (2016), "Performance-based seismic design of flexible-base multi-storey buildings considering soil–structure interaction," *Engineering Structures* **108**(1) 90-103.

[10] Ganjavi, B., Hajirasouliha I., and Bolourchi, A. (2016), "Optimum lateral load distribution for seismic design of nonlinear shear-buildings considering soil-structure interaction," S*oil Dynamics and Earthquake Engineering* **88:** 356-368.

[11] Hussien, M. N., Tobita, T., Iai, S. and Mourad Karray (2016), "Soil-pile-structure kinematic and inertial interaction observed in geotechnical centrifuge experiments," *Soil Dynamics and Earthquake Engineering,* **89**: 75-84.

[12] Etedali, S., Seifi, M. and Akbari, M. (2018), A numerical study on optimal FTMD parameters considering soil-structure interaction effects, *Geomechanics and Engineering*, **16**(5).

[13] Rahai, A. R., Saberi, H. and Saberi, H. (2017), "A Discussion of the paper: "Ant colony optimization of tuned mass dampers for earthquake oscillations of high-rise structures including soil–structure interaction," [Soil Dynamics and Earthquake Engineering. **51** (2013) 14–22]" *Soil Dynamics and Earthquake Engineering* **102**: 263-265.

[14] Nazarimofrad, E. and Zahrai, S. M. (2016), "Seismic control of irregular multistory buildings using active tendons considering soil–structure interaction effect," *Soil Dynamics and Earthquake Engineering* **89**: 100-115.

[15] Sharmin, F., Hussan, M., Kim, D. and Gook Cho, S. (2017), "Influence of soil-structure interaction on seismic responses of offshore wind turbine considering earthquake incident angle," *Earthquakes and Structures*, **13**(1).

[16] Zhou, F., Liu, H., Mori, M., Nobuo, F. and Zhu, H. (2016), "Seismic response of a continuous foundation structure supported on partially improved foundation soil," *Soil Dynamics and Earthquake Engineering,* **90**: 128-137.

[17] Gičev, V., Trifunac, M. D. and Orbović, N. (2016), "Two-dimensional translation, rocking, and waves in a building during soil-structure interaction excited by a plane earthquake SV-wave pulse," *Soil Dynamics and Earthquake Engineering,* **88**: 76-91.

[18] Liang, J., Jin, L., Todorovska, M, I. and Trifunac, M. D. (2016), "Soil–structure interaction for a SDOF oscillator supported by a flexible foundation embedded in a half-space: Closed-form solution for incident plane SH-waves," *Soil Dynamics and Earthquake Engineering* **90**: 287-298.

[19] Tabatabaei Mirhosseini R. (2017), "Seismic response of soil-structure interaction using the support vector regression," *Structural Engineering and Mechanics*, **63**(1).

[20] He, C., Zhou, S., Di, H. and Shan, Y. (2017), "A 2.5-D coupled FE–BE model for the dynamic interaction between saturated soil and longitudinally invariant structures," *Computers and Geotechnics,* **82:** 211-222.

[21] Amorosi, A., Boldini, D. and di-Lernia, A. (2017), "Dynamic soil-structure interaction: A three-dimensional numerical approach and its application to the Lotung case study," *Computers and Geotechnics,* **90**: 34-54.

[22] Bin Ali, S. and Kim, D. (2017), "Wavelet analysis of soil-structure interaction effects on seismic responses of base-isolated nuclear power plants," *Earthquakes and Structures*, **13**(6).

[23] Messioud, S., Sbartai, B. and Dias, D. (2016), "Seismic response of a rigid foundation embedded in a viscoelastic soil by taking into account the soil-foundation interaction," Str*uctural Engineering and Mechanics*, **58**(5) 5.

[24] Rahmani, A. Taiebat, M., Liam Finn, W.D. and Ventura, C. E. (2016), "Evaluation of substructuring method for seismic soil-structure interaction analysis of bridges," *Soil Dynamics and Earthquake Engineering* **90**: 112-127.

[25] Yu, Y., Damians, I.P. and Bathurst, R. J. (2015), "Influence of choice of FLAC and PLAXIS interface models on reinforced soil–structure interactions," *Computers and Geotechnics* **65**: 164-174.

[26] Torabi, H., and Rayhani, M.T. (2014), "Three dimensional Finite Element modeling of seismic soil–structure interaction in soft soil," *Computers and Geotechnics* **60:** 9-19.

[27] Jahangir, E., Deck, O. and Masrouri, F. (2013), "An analytical model of soil–structure

interaction with swelling soils during droughts," *Computers and Geotechnics* **54**: 16-32.

[28] Ghandil, M., Behnamfar, F. and Vafaeian, M. (2016), "Dynamic responses of structure–soil–structure systems with an extension of the equivalent linear soil modeling," *Soil Dynamics and Earthquake Engineering,* **80**: 149-162.

[29] Aldaikh, H., Alexander, N.A., Ibraim, E. and Knappett, J. (2016), "Shake table testing of the dynamic interaction between two and three adjacent buildings (SSSI)," *Soil Dynamics and Earthquake Engineering,* **89**: 219-232.

[30] Aldaikh, H., Alexander, N. A., Ibraim, E. and Oddbjornsson, O. (2015), "Two dimensional numerical and experimental models for the study of structure–soil–structure interaction involving three buildings," *Computers & Structures*, **150**(1): 79-91.

[31] Álamo, G. M., Padrón, L. A., Aznárez, J.J. and Maeso, O. (2015), "Structure-soil-structure interaction effects on the dynamic response of piled structures under obliquely incident seismic shear waves," *Soil Dynamics and Earthquake Engineering* **78**: 142-153.

[32] Madani, B., Behnamfar, F., and Riahi, H.T. (2015), "Dynamic response of structures subjected to pounding and structure–soil–structure interaction," *Soil Dynamics and Earthquake Engineering* **78**: 46-60.

[33] Roy, C., Bolourchi, S. and Eggers, D. (2015), "Significance of structure–soil–structure interaction for closely spaced structures," N*uclear Engineering and Design* **295**(15): 680-687.

[34] Trombetta, N.W., Mason, H.B., Chen, Z., Hutchinson, T.C., Bray, J.D. and Kutter, B.L. (2013), "Nonlinear dynamic foundation and frame structure response observed in geotechnical centrifuge experiments," *Soil Dynamics and Earthquake Engineering* **50**: 117-133.

[35] Mason, H.B., Trombetta, N.W., Chen, Z., Bray, J.D., Hutchinson, T.C. and Kutter, B.L. (2013), "Seismic soil–foundation–structure interaction observed in geotechnical centrifuge experiments," *Soil Dynamics and Earthquake Engineering* **48:** 162-174.

[36] Wang, H.F., Lou, M.L., Chen, X. and Zhai, Y.M. (2013), "Structure–soil–structure interaction between underground structure and ground structure," *Soil Dynamics and Earthquake Engineering* **54**: 31-38.

[37] Menglin, L., Huaifeng, W., Xi C., and Yongmei, Z. (2011), "Structure–soil–structure interaction: Literature review" *Soil Dynamics and Earthquake Engineering,* **31**(12): 1724-1731.

[38] Padrón, L.A., Aznárez, J. J. and Maeso, O. (2009), "Dynamic structure–soil–structure interaction between nearby piled buildings under seismic excitation by BEM–FEM model," *Soil Dynamics and Earthquake Engineering* **29**(6): 1084-1096.

[39] Wolf, J. P. (1985), Dynamic soil-structure interaction, Englewood Cliffs, NJ, Prentice-Hall.

[40] Wolf, J. P. (1988), Soil-structure interaction analysis in time domain, Englewood Cliffs, NJ, Prentice-Hall.

[41] Kramer, S. L. (1996), Geotechnical earthquake engineering, Simon & Schuster, NJ, Prentice-Hall.

[42] Ruiz-Pinilla, J.G., Pallarés, F.J., Gimenez, E. and Calderón, P.A. (2014), Experimental tests on retrofitted RC beam-column joints underdesigned to seismic loads. General approach, *Engineering Structures*, **59**: 702-714.

[43] Yarahmadi, M., Baghlani, A. and JavidSharifi, B. (2015), Optimum retrofit of a 3-story RC frame considering non-linear SSI, *the 7th International Conference on Seismology and Earthquake Engineering (SEE7)*, the International Institute of Earthquake Engineering & Engineering Seismology (IIEES), Tehran, Iran.

[44] Yarahmadi, M., Baghlani, A. and JavidSharifi, B. (2015), CFRP-retrofitting of reinforced concrete frames considering non-linear soil-structure interaction, *the 7th International Conference on Seismology and Earthquake Engineering (SEE7)*, the International Institute of Earthquake Engineering & Engineering Seismology (IIEES), Tehran, Iran.

[45] Kanbur, Ali Fuat Genc and Ebru Kalkan (2019), Structural response of historical masonry arch bridges under different arch curvature considering soil-structure interaction, G*eomechanics and Engineering*, **18**(2).

[46] Cosenza, E., Manfredi, G. and Verderame, G.M (2006), A fibre model for push-over analysis of underdesigned reinforced concrete frames, Computers & Structures, 84(13, 14): 904-916.

[47] Fatahi, B., Tabatabaiefar, S.H.R. and Samali, B. (2014), soil-structure interaction vs Site effect for seismic design of tall buildings on soft soil, *Geomechanics and Engineering*, **6**(3).

[48] Mazzoni, S., McKenna, F., Scott, M. H., Fenves, G.L. (2007), OpenSees Command Language Manual of Modeling and Analysis of Structural Systems.

[49] Neuenhofer, A., Filippou, F.C. (1998), "Geometrically Nonlinear Flexibility-Based Frame Finite Element," *ASCE Journal of Structural Engineering*, **124**(6): 704-711, ISSN 0733-9445/98/0006-0704-0711, Paper 16537.

[50] Neuenhofer, A., Filippou, F.C. (1997), Evaluation of Nonlinear Frame Finite-Element Models. *ASCE Journal of Structural*

Engineering, **123**(7): 958-966, ISSN 0733-9445/97/0007-0958-0966. Paper No. 14157.

[51] Taucer, F.F., Spacone, E. and Filippou, F.C. (1991) "A Fiber Beam-Column Element for Seismic Response Analysis of Reinforced Concrete Structures," Report No. UCB/EERC-91/17. Earthquake Engineering Research Center, College of Engineering, University of California, Berkeley.

[52] Khazaei, J., Amiri, A. and Khalilpour, M. (2017), "Seismic evaluation of soil-foundation-structure interaction: Direct and Cone model," *Earthquakes and Structures*, **12**(2).

[53] Lashkari, A., (2010) "A SANISAND model with anisotropic elasticity," *Soil Dynamics and Earthquake Engineering*, (**30**)12: 1462-1477.

[54] Yang, Z., Elgamal, A. and Parra, E. (2003) "Computational Model for Cyclic Mobility and Associated Shear Deformation," *Geotechnical and Geo-environmental Engineering, ASCE*, **129**(12): 1119-1127.

[55] Elgamal, A., Yang, Z., Parra E. and Ragheb, A. (2003), "Modeling of Cyclic Mobility in Saturated Cohesionless Soils," *International Journal of Plasticity*, **19**(6): 883-905.

[56] Yang, Z. and Elgamal, A. (2002), "Influence of Permeability on Liquefaction-Induced Shear Deformation," *Engineering Mechanics, ASCE,* **128**(7): 720-729.

[57] Elgamal, A., Yang Z. and Parra, E. (2002), "Computational Modeling of Cyclic Mobility and Post-Liquefaction Site Response," *Soil Dynamics and Earthquake Engineering*, **22**(4): 259-271.

[58] Yang, Z. (2000), "Numerical Modeling of Earthquake Site Response Including Dilation and Liquefaction," PhD Thesis, Dept. of Civil Engineering and Engineering Mechanics, Columbia University, NY, New York.

[59] Parra, E. (1996), "Numerical Modeling of Liquefaction and Lateral Ground Deformation Including Cyclic Mobility and Dilation Response in Soil Systems," PhD Thesis, Dept. of Civil Engineering, Rensselaer Polytechnic Institute, Troy, NY.

[60] Kuhlemeyer, R. L. & Lysmer, J. (1973) "Finite element method accuracy for wave propagation problems," *Journal of Soil Mechanics & Foundations*, Div, 99.

[61] Lysmer, I., Udaka, T., Tsal, C.F. and Seed, H.B. (1975) "FLUSH: a computer program for approximate 3-D analysis of soil-structure interaction problems," Report EERC 75-30, Earthquake Engineering Research Center, University of California, Berkeley, page 83.

[62] Seed, H. B., Murarka, R., Lysmer, J. & Idriss, I. (1976) "Relationships of maximum acceleration, maximum velocity, distance from source, and local site conditions for moderately strong earthquakes," *Bulletin of the Seismological Society of America*, **66**: 1323-1342.

[63] Tabatabaiefar, H. R., & Fatahi, B. (2014), "Idealisation of soil–structure system to determine inelastic seismic response of mid-rise building frames," *Soil Dynamics and Earthquake Engineering* **66**: 339–351.

[64] Karapetrou, Fotopoulou, and Pitilakis (2015) "Seismic vulnerability assessment of high-rise non-ductile RC buildings considering soil–structure interaction effects," *Soil Dynamics and Earthquake Engineering*, **73**: 42–57.

[66] Lysmer, J., & Kuhlemeyer, R. (1969) "Finite dynamic model for infinite media". *Journal of the Engineering Mechanics Division*, *Proc. ASCE*, **95**(4), 859 – 876.

[66] ACI 318 (2014), Building Code Requirements for Structural Concrete (ACI 318-14) and Commentary (ACI 318R-14), ACI Committee 318, *American Concrete Institute, Farmington Hills*, MI.

[67] Gazetas, G., Anastasopoulos, I. and Garini, E. (2014), "Geotechnical design with apparent seismic safety factors well-bellow 1," *Soil Dynamics and Earthquake Engineering* **57**: 37–45.

[68] Crouse, C. B. and Ramirez, J. C. (2003), "Soil-Structure Interaction and Site Response at the Jensen Filtration Plant during the 1994 Northridge, California, Mainshock and Aftershocks," *Bulletin of the Seismological Society of America*, **93**(2): 546–556.

[69] Stewart, J. P., Seed, R. B. and Fenves G. L. (1998), "Empirical Evaluation of Inertial Soil-Structure Interaction Effects," Pacific Earthquake Engineering Research Center, Report No. PEER-98/07, University of California Berkeley, California.

[70] NEHRP Consultants Joint Venture (2012), "Soil-Structure Interaction for Building Structures," U.S. Department of Commerce National Institute of Standards and Technology Engineering Laboratory Gaithersburg, MD 20899, NIST GCR 12-917-21.

[71] Minimum Design Loads for Buildings and Other Structures, American Society of Civil Engineers, ASCE/SEI 7-10.